JOURNAL OF GUIDANCE, CONTROL, AND DYNAMICS
Vol. 25, No. 3, May–June 2002

Robust H_2 Design for Lateral Flight Control of Highly Flexible Aircraft

Daniel Alazard*
ONERA, 31055 Toulouse, France

A lateral flight control design for a flexible aircraft is presented. It is based on a standard two-input–two output problem formalism and H_2 synthesis. The proposed approach consists of two steps. The first step deals with the synthesis of a dynamic output feedback satisfying modal specifications on the rigid modes, stability requirements on the structure, and performance robustness with respect to the various loading cases. The originality in the synthesis setup proposed is that it combines eigenstructure assignment, H_2 frequency domain synthesis, and parametric robustness design. The second step uses a recent theoretical result to transform a given compensator into a linear quadratic Gaussian compensator involving a judiciously selected onboard model. The two-degree-of-freedom compensator thus obtained allows time-domain specifications in response to the pilot's commands to be met satisfactorily. A detailed discussion is provided of the approach together with the aircraft models used and corresponding closed-loop analysis.

Introduction

FLEXIBLE structures give rise to many control problems and are particularly relevant applications for the evaluation of control law synthesis techniques and algorithms. Frequency-domain synthesis techniques (H_∞, H_2) are suitable to handle rolloff specifications required to prevent spill over on the flexible modes, which are neglected in the synthesis model.[1] Additionally, to prevent pole/zero cancellation,[2] it is necessary to take into account parametric uncertainties on the flexible modes to be controlled, that is, uncertainties related to modes whose natural frequencies are within the bandwidth of the loop transfer $L(s) = K(s)G(s)$. The techniques of μ synthesis[1] or parametric robust linear quadratic Gaussian (PRLQG) synthesis[3] are good candidates for parametric robustness specifications. On the other hand, these frequency-domain or quadratic-type techniques are less suitable when the time domain or modal specifications (eigenvalue assignment, decoupling) on the rigid modes of the system are required. The latter point is particularly significant within the context of flight control laws and more particularly the roll/yaw decoupling required for lateral flight.[4] The synthesis task is actually a multiobjective synthesis problem. Explicit model following methods can be used to take into account decoupling requirements in the framework of optimal synthesis techniques,[5] but these approaches, by increasing the order of the (augmented) plant, also increase the order of the compensator when dynamic output feedback is required. Sato and Suzuki propose an interesting approach that combines an H_∞ estimator and a state feedback gain designed by eigenstructure assignment to overcome this difficulty.[6] More generally, the combination of eigenstructure assignment and quadratic techniques is often mentioned in aeronautical applications.[7–9] Implicit model following design is an alternative to mix eigenstructure assignment on a reduced-order model and linear quadratic regulation on a full-order model.[10] In the same manner, the "cross standard form" we propose in this paper is a competitive technique to combine eigenstructure assignment and optimal (H_2 or H_∞) syntheses.

In addition, it could be worthwhile to test different sensor configurations. Namely, it must be possible to modify the measurement vector in the model without any adjustments of the synthesis procedure, thus allowing direct analysis of the influence of the sensors on closed-loop behavior. The traditional block diagrams of mixed sensitivity or loop shaping are too weak to handle such constraints. The synthesis structure we present here has been developed to take into account various specifications (modal, frequency domain, parametric robustness) and to evaluate various sensor configurations. These evaluations are not presented in this paper due to the lack of space.

Finally, another point treated in this paper is feedforward control. Output feedback is generally designed on modal specifications, disturbance rejection specifications, and robustness specifications. However, the responses to the pilot's commands and their transient shapes (time-domain specifications) are crucial within the context of flight control systems and require a feedforward law.[11] We propose a new approach for dynamic feedforward synthesis based on the equivalent LQG structure.[12]

The first part of this paper outlines the models and the specifications. The second part deals with model analysis and reduction. It proposes an approach combining the balanced reduction and an analysis of the participation of flexible modes in the system fed back by the rigid control law.[13] The third part is the most important one and is devoted to robust dynamic output feedback synthesis. Two syntheses are presented: The first design is based on the rigid model and only aims to satisfy the performances on the rigid modes and the stability of the flexible modes; the second design specially handles flexible mode damping. These modes are explicit parts of the synthesis model to meet the requirements of comfort during turbulence. In the final part, the nominal compensator is expressed as a two-degree-of-freedom LQG compensator to improve response to pilot's commands.

Models and Specifications

The models used in this study are linearized models of the lateral motion of a flexible aircraft around equilibrium points. The system is a large carrier aircraft in which flexibility was intentionally degraded to evaluate the relevance of control law synthesis techniques in highly critical cases. The models† are 60th-order state-space representations with 2 control inputs (aileron deflection ∂_l and rudder deflection ∂_n) and 44 measurements: 4 measurements (lateral acceleration n_{yi}, roll rate p_i, yaw rate r_i, and roll angle ϕ_i) at 11 measurement points regularly spaced along the fuselage ($i = 1, \ldots, 11$). The state vector $\boldsymbol{x}$ contains 4 rigid states (yaw angle β, roll rate p, yaw rate r, and roll angle ϕ), 36 states corresponding to 18 flexible modes modeled between 8 and 80 rad/s (generalized coordinates q_j

Received 1 August 2000; revision received 14 July 2001; accepted for publication 10 August 2001.

*Research Engineer, Department of System Control and Flight Dynamics, 2 Avenue Edouard Belin; also Professor, Automatic Control Department, SUPAERO.

†The reader will find the MATLAB® source files required to load these models and to run the main results presented in this paper online at http://www.cert.fr/fr/dcsd/CDIN/CDINPUB/alazard/AIAA_JGCD/[cited 26 October 2001].

and $\dot{q}_j$, $j = 1, \ldots, 18$), and 20 secondary states that represent the dynamics of the servocontrol surfaces and aerodynamic lags.

The models are available for three different flight conditions and six different loading cases (corresponding to six distributions of the mass inside the plane). The results presented involve only two models under one flight condition (a light model noted G_1 and a heavy model noted G_2). We will also refer to the corresponding rigid models (G_1^r and G_2^r) in which only the four rigid states ($\boldsymbol{x}_r = [\beta, p, r, \phi]^T$) are considered.

Let us denote the state-space representation of a model $G_i^j(s)$:

$$G_i^j(s) \equiv \left[\begin{array}{c|c} A_i^j & B_i^j \\ \hline C_i^j & D_i^j \end{array}\right] \tag{1}$$

The following list summarizes the various specifications:

Dutch roll damping ratio >0.5, S1; templates on the step responses with respect to β and p, S2; roll/yaw channel decoupling, S3; no degradation of the damping ratios of flexible modes, or, furthermore, an increase of the damping ratios of low-frequency flexible modes to improve comfort during turbulence, S4; previous performances must be robust with respect to the various loading cases, S5; and use a reasonable number of measurements (between 4 and 10), S6.

The last specification S6 is not common for control law designers. Actually, the problem of sensor selection is not so independent of the control design and depends on the control law objectives: If there are no specifications on the damping of a structural mode (passive synthesis), it is interesting to place gyrometers on a vibration antinode and a linear accelerometer on a vibration node. If we want to damp this mode (active synthesis), this choice is arguable. If redundant sensors can be used in various locations and if parametric robustness requirements are taken into account, this problem becomes very hard. Therefore, a design in which the tunings depend only on the control objectives, not on the measurements used, can be a very powerful tool.

Modal and time-domain specifications (S1–S3) involve the rigid dynamics of the aircraft. If the system is assumed to be rigid, eigenstructure assignment techniques are particularly effective at handling these specifications, especially because we have a sufficient number of outputs ($\geq$4) to implement an ideal rigid state feedback by a static output feedback. These techniques will not be detailed in this paper.[14] A rigid state feedback K_{x_r} on the four rigid states $\boldsymbol{x}_r$ was thus calculated on model G_1^r to meet the following modal specifications (see Chap. 8, pt. 3 in Ref. 4):

1) The Dutch roll mode is damped and assigned to $-1 + 1.3i$ and is decoupled from ϕ.

2) The pure roll mode is assigned to -1.1 and is decoupled from β (that is, the natural dynamics is preserved).

3) The spiral mode is assigned to -1 and is decoupled from β: This mode is naturally very slow, even unstable on the heavy model. This assignment aims to accelerate its dynamics up to 1 rad/s to meet pilot's requirements and control effort specifications independently of feedforward control laws.

Note that eigenstructure assignment involves the rigid dynamics, not the flexible dynamics . Although flexible mode damping could be easily handled by eigenstructure design, such a design might lead to undesirable high efforts on control surfaces. Thus, we have chosen to handle flexible mode control by an H_2 design (see section "Active Synthesis").

Time responses obtained on the rigid model G_1^r are presented in Fig. 1 (black curve). These responses satisfy (S1–S3) and will be used as a reference to appreciate the solutions proposed on the full-order models. This simulation plots the rigid state responses $\beta(t)$, $\phi(t)$, $p(t)$, and $r(t)$ to β_{ref} and p_{ref} step inputs. In fact, the actual command that is applied is

$$\begin{bmatrix} \partial_l \\ \partial_n \end{bmatrix} = H \begin{bmatrix} \beta_{\text{ref}} \\ \dfrac{1}{s}\, p_{\text{ref}} \end{bmatrix} - K_{x_r} \boldsymbol{x}_r \tag{2}$$

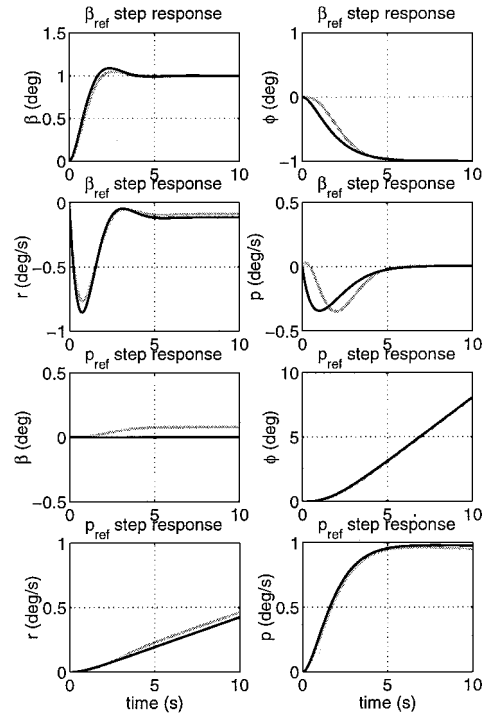

Fig. 1 Nominal rigid simulations: G_1^r (black) and G_2^r (gray).

where H is a feedforward static matrix computed to ensure the steady-state constraint

$$\lim_{t \to \infty} \begin{bmatrix} \beta(t) \\ \phi(t) \end{bmatrix} = \begin{bmatrix} 1 & 0 \\ -1 & 1 \end{bmatrix} \begin{bmatrix} \beta_{\text{ref}} \\ \dfrac{1}{s}\, p_{\text{ref}} \end{bmatrix} \tag{3}$$

One can also observe in Fig. 1 that the responses obtained on G_2^r (grey curve) are satisfactory (robustness specification S5). Thus, there is no robustness problem if the specifications and models are limited to the rigid aircraft behavior, and the problem can now be restated in the following manner:

1) Synthesize a control law satisfying the frequency domain and modal specifications S4 on the flexible modes,

2) Preserve as much as possible the rigid performances obtained with the modal gain K_{x_r}.

The whole process must be carried out under the robustness requirement S5 and the hardware constraint S6.

Model Analysis and Reduction

To evaluate the various syntheses, we will also analyze the root locus of the loop transfer $L(s) = K(s)G(s)$ obtained while varying feedback gains from 0 to 1 simultaneously on both control channels ∂_l and ∂_n (see Fig. 2 as an example; $\times$ and $+$ indicate open-loop and closed-loop poles, respectively). Such a root locus is a powerful graphical tool to verify that the rigid modes are correctly assigned, that no flexible mode is destabilized (Fig. 3), and that critical flexible modes are damped (Fig. 4). These root loci are plotted in the vicinity of the imaginary axis and on a reduced frequency range (0–40 rad/s): the servo-control dynamics (around 6 Hz) are not inside this window. Note the very low-frequency dynamics on the real axis (aerodynamic lags).

The number of measurements is higher than the number of rigid states. Therefore, it is easy to compute the static output feedback K_y that is equivalent to the state feedback K_{x_r},

$$K_y = K_{x_r}\left(C_1^r - D_1^r K_{x_r}\right)^+ \tag{4}$$

with the pseudoinverse notation (least-square solution):

$$A^+ = (A^T A)^{-1} A^T \tag{5}$$

C_1^r and D_1^r are the output and direct feedthrough matrices of model G_1^r restricted to the only measurements used. If we consider only

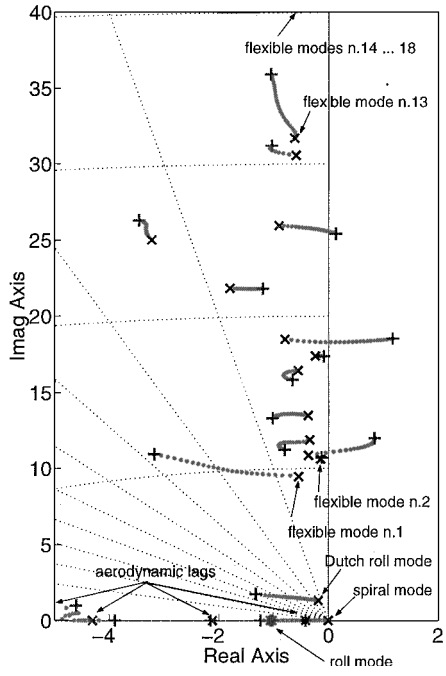

Fig. 2 $K_{y6}G_1(s)$**: root locus.**

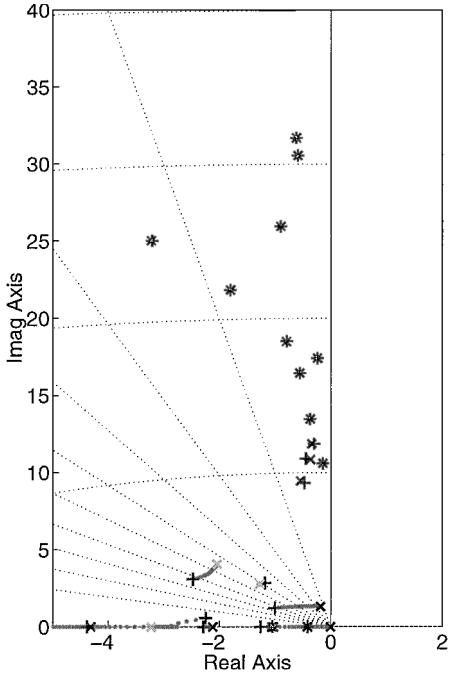

Fig. 3 $-K_0(s)G_1(s)$**: root locus.**

the four measurements n_{y_i}, p_i, r_i, and ϕ_i at the measurement point i, we will note these matrices C^r_{1i} and D^r_{1i} and the resulting gain K_{y_i}.

We can then evaluate the couplings between rigid dynamics and flexible dynamics by plotting the root locus of the loop obtained when this output feedback K_y is applied to the full model G_1 or G_2. Such root loci have been performed for the 11 measurement points, $K_{y_i}, i = 1, \ldots, 11$. This analysis highlights that, in all cases, the static output feedback designed to assign the rigid modes destabilizes the flexible modes and that the rigid/flexible dynamic couplings are less significant when the measurements at the aircraft center, K_{y_6}, are used (Fig. 2):

1) The trajectories of the flexible poles are less significant in the right-half plane,

2) The prescribed assignment on the rigid modes is clearly perturbed by dynamic couplings when extreme measurement points are used, K_{y1} or K_{y11}, particularly in the case of model $G_2(s)$ (heavy

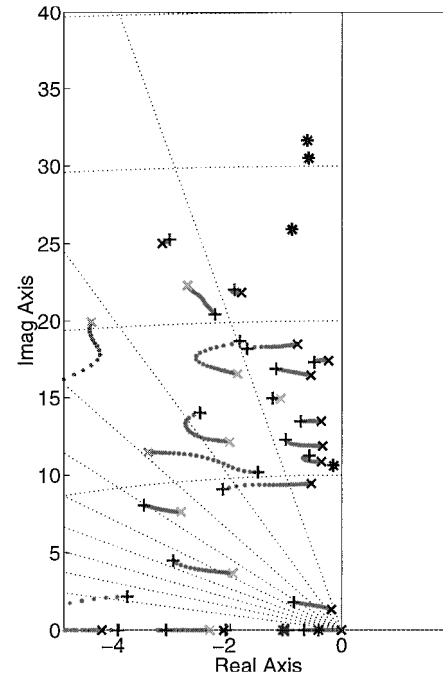

Fig. 4 $-K_1(s)G_1(s)$**: root locus.**

case), where the Dutch roll mode becomes unstable. Furthermore, in the case of measurements at the aircraft center, the trajectories from the rigid modes are insensitive to the loading case. This shows that the measurement location with respect to the vibration nodes is a critical factor for the stability of the various flexible and rigid modes.

It can also be seen that some flexible modes, particularly the flexible mode 2 (in order of increasing pulsations), are insensitive to the various feedbacks K_{yi}: The later are local modes that are almost uncontrollable by the control inputs ∂_l and ∂_n. These modes should, therefore, be reduced in the synthesis model.

Finally, we will also consider this root locus-based analysis of rigid/flexible coupling, to evaluate how meaningful the reduced-order models are with respect to the control law synthesis problems. The model will be reduced as long as the shape of the root locus obtained with the reduced model is qualitatively preserved. Flexible modes and secondary modes have to be reduced in separate ways. From a real block-diagonal realization, the flexible modes are reduced by visual selection, the subspace associated with the secondary modes is balanced and truncated. The four rigid modes $\boldsymbol{x}_r$ are systematically preserved. The reduced-order synthesis model thus obtained is noted $G(s)$. Figure 5 shows the root locus obtained from a second-order reduction of the secondary dynamics (the corresponding states are noted $\boldsymbol{x}_p = [x_p^1, x_p^2]^T$) and from the elimination of flexible modes 2, 14, 15, 16, 17, and 18 on model G_1. The resulting model $G(s)$ is thus a 30th-order model associated with the state vector:

$$\boldsymbol{x} = \left[\boldsymbol{x}_r^T, \boldsymbol{x}_p^T, \ldots, q_j, \dot{q}_j, \ldots\right]^T, \qquad j = 1,\ 3,\ 4, \ldots,\ 13 \quad (6)$$

It can be observed in Fig. 5, by comparison with Fig. 2, that the reduced model $G(s)$ is quite representative of dynamic couplings up to 30 rad/s. Beyond this pulsation, some sensitive flexible modes have been neglected and should be gain controlled. Thus, it will be necessary to take into account a rolloff specification to prevent spill over on these modes.

The number of significant low-frequency flexible modes we wish to preserve in the synthesis model strongly depends on the control law objectives.

1) In the case of a control law with a weak action on the flexible modes, only the first flexible modes, if any, shall be preserved (see section "Passive Synthesis"),

2) In the case of a very active law that aims at damping the flexible modes in a given bandwidth, it will be necessary to keep all of the sensitive modes in this bandwidth as well as some other modes to prevent side effects (see section "Active Synthesis").

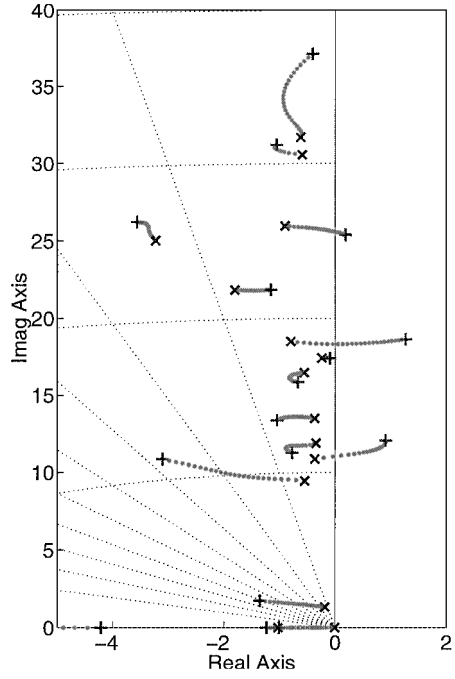

Fig. 5 $K_{y6}G(s)$**: root locus.**

Output Feedback Synthesis by Multiobjective H_2 Design

Cross Standard Form

The cross standard form we detail in this section is based on the structure of LQG compensators and more generally on compensators involving a state observer (with an estimation gain K_f) and a state feedback (with a gain K_c).

Let us consider a system defined by the general state representation (n states, m commands, and p outputs):

$$\left[\begin{array}{c}\dot{x}\\ \hline y\end{array}\right] = \left[\begin{array}{c|c} A & B \\ \hline C & D\end{array}\right]\left[\begin{array}{c} x \\ \hline u\end{array}\right] \tag{7}$$

and the standard problem $P_p(s)$ called cross standard form, associated with this system is

$$P_p(s):\left[\begin{array}{c}\dot{x}\\ \hline z\\ \hline y\end{array}\right] = \left[\begin{array}{c|c|c} A & K_f & B \\ \hline K_c & 0 & I_m \\ \hline C & I_p & D\end{array}\right]\left[\begin{array}{c} x \\ \hline w \\ \hline u\end{array}\right] \tag{8}$$

where K_c and K_f indicate, respectively, a state feedback gain and a state estimation gain both synthesized to meet some specifications using a suitable technique (modal, LQG, etc.). We will also assume that $A - BK_c$ and $A - K_fC$ are stable.

H_2 and H_∞ syntheses carried out on the problem $P_p(s)$ provide the same solution. This solution coincides with the LQG compensator [noted $K_{\mathrm{LQG}}(s)$] built on K_c and K_f is

$$\left[\begin{array}{c}\dot{\hat{x}}\\ \hline u\end{array}\right] = \left[\begin{array}{c|c} A - BK_C - K_fC + K_fDK_c & K_f \\ \hline -K_c & 0\end{array}\right]\left[\begin{array}{c} \hat{x} \\ \hline y\end{array}\right] \tag{9}$$

Justification

The state representation of the augmented system $P_p(s)$ fed back by the compensator $K_{\mathrm{LQG}}(s)$, that is, $F_l[P_p(s), K_{\mathrm{LQG}}(s)]$, is

$$\left[\begin{array}{c}\dot{x}\\ \dot{\hat{x}}\\ \hline z\end{array}\right] = \left[\begin{array}{cc|c} A & -BK_c & K_f \\ K_fC & A - BK_c - K_fC & K_f \\ \hline K_c & -K_c & 0\end{array}\right]\left[\begin{array}{c} x \\ \hat{x} \\ \hline w\end{array}\right] \tag{10}$$

Let us carry out the change of variable using the estimation error $\varepsilon_x = x - \hat{x}$:

$$\left[\begin{array}{c} x \\ \hat{x}\end{array}\right] = \mathcal{M}\left[\begin{array}{c} x \\ \varepsilon_x\end{array}\right] \quad \text{with} \quad \mathcal{M} = \left[\begin{array}{cc} I_n & 0 \\ I_n & -I_n\end{array}\right] \tag{11}$$

The new representation of $F_l[P_p(s), K_{\mathrm{LQG}}(s)]$ is

$$\left[\begin{array}{c}\dot{x}\\ \dot{\varepsilon}_x\\ \hline z\end{array}\right] = \left[\begin{array}{cc|c} A - BK_c & BK_c & K_f \\ 0 & A - K_fC & 0 \\ \hline 0 & K_c & 0\end{array}\right]\left[\begin{array}{c} x \\ \varepsilon_x \\ \hline w\end{array}\right] \tag{12}$$

Note that the states ε_x associated with the estimation error are uncontrollable by w and that the plant states x are unobservable by z. The transfer between w and z, therefore, vanishes:

$$F_l[P_p(s), K_{\mathrm{LQG}}(s)] = 0 \tag{13}$$

and, consequently,

$$\|F_l(P_p(s), K_{\mathrm{LQG}}(s))\|_2 = \|F_l(P_p(s), K_{\mathrm{LQG}}(s))\|_\infty = 0 \tag{14}$$

This compensator, K_{LQG}, is thus the optimal solution of the standard problem $P_p(s)$ in H_2 and H_∞ norm senses.

Practical Use

This result can be considered as a generalization, for H_2 and H_∞ criteria, of the solution to the LQ inverse problem, raised in the 1960s and 1970s, which consisted in finding the LQ cost whose minimization restores a given state feedback. This cross standard form used as such is not of interest because it is necessary to know gains K_c and K_f to set up the problem $P_p(s)$ and finally to find the initial LQG compensator. On the other hand, from a state feedback K_c satisfying some time-domain specifications, the cross standard form can be very useful to initialize a standard setup that will be completed by dynamic weightings to take into account frequency-domain specifications. If the Kalman filter gain K_f is not specified, the cross standard form becomes the well-known output estimation (OE) problem and is:

$$P_{\mathrm{OE}}(s) := \left[\begin{array}{c|c|c} A & B_1 & B \\ \hline K_c & 0 & I \\ \hline C & D_{21} & D\end{array}\right] \tag{15}$$

It can then be shown [see Ref. 15 for proof and standard notations in Eq. (15)] that the H_2 or H_∞ optimal compensator on this problem assigns n closed-loop eigenvalues of the matrix $A - BK_c$.

In our application, we computed a state feedback gain,

$$K = \left[K_{x_r},\, 0, \ldots, 0\right] \tag{16}$$

on the state x of the reduced model G [see Eq. (6)]. It is designed to assign the four rigid modes. The synthesis setup to be used is presented in Fig. 6 and can be clarified as follows:

1) A controlled output $z_1 = u + Kx$ is used to inflect the synthesis toward the nominal rigid solution.

2) A controlled output z_2 is used to specify an rth-order rolloff beyond the pulsation ω.

3) Very low measurement noises w_1 ($\varepsilon = 0.001$) are used because the number of measurements is high enough to estimate directly and statically the rigid states. This tuning leads to very fast dynamics in the compensator, which can be reduced after the synthesis,

4) Initial conditions w_2 are used on the four rigid states ($V = [I_{4\times 4},\, 0, \ldots, 0]$).

The output z_2 actually weights the rth derivative of the control signal u. This rolloff formulation is interesting because it does not require specification of the cutoff shape as in the case of high-pass filters usually introduced on the control signal. The open loop feed-through transfer between u and $[z_1\ z_2]^T$ reads $[1\ (s/\omega)^r]^T$. [This rough calculus does not take into account the fast poles

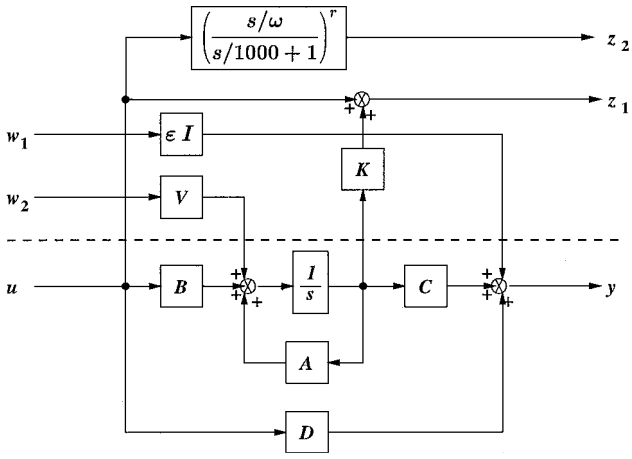

Fig. 6 Setup for rolloff and rigid performances.

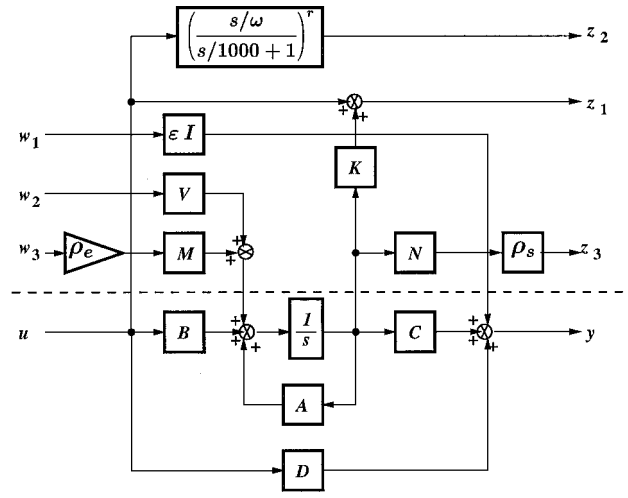

Fig. 7 Setup for active synthesis.

(−1000 rad/s) introduced in the pseudo-derivation]. The singular value of this transfer exhibits the required rolloff characteristics, that is, a unitary gain in low frequency and a slope of $20r$ dB/decade beyond the pulsation ω. Finally, it may seem surprising that the rolloff specification was not introduced on the measurement noises even though doing so would have allowed the output z_2 to be removed and the problem to be an exact OE problem [Eq. (15)]. The reason is simple. Because there are more measurements than control inputs and because the set of measurements must be eventually modified (4–10 measurements among 44), we chose to introduce the rolloff specification on the control inputs rather than on the measurements to 1) reduce the problem dimension and, therefore, the compensator order (in Fig. 6, there are as many filters $[s/\omega/(s/1000+1)]^r$ as control inputs, that is, two), and 2) get a tuning independent of measurements because the only tuning parameter of the setup that would require modification due to a new set of measurements is the size of the measurement noise $\boldsymbol{w}_1$. Its weight is marginal (εI), and its impact on the synthesis will be masked by truncating the fast poles of the compensator.

Passive Synthesis

The passive synthesis consists in applying the earlier synthesis setup (Fig. 6) to the rigid model $G_1^r(s)$ with four measurements at the aircraft center, $(i = 6)$, that is,

$$\left[\begin{array}{c|c} A & B \\ \hline C & D \end{array}\right] = \left[\begin{array}{c|c} A_1^r & B_1^r \\ \hline C_{16}^r & D_{16}^r \end{array}\right], \qquad K = K_{xr}, \qquad V = I_{4\times 4} \tag{17}$$

and in increasing r and decreasing ω until the compensator stabilizes the full-order model $G_1(s)$. In fact, starting with $r = 2$, we decrease ω as long as the rigid pole assignment is not too perturbed, then we increase r if ω is too close to the rigid mode pulsations. The choice

$$r = 3, \qquad \omega = \pi \text{ rad/s} \qquad (0.5 \text{ Hz}) \tag{18}$$

leads to an interesting solution. The order of this problem, and consequently the order of the compensator, is $10\,(4 + 2 \times 3)$. This compensator $K_0(s)$ exhibits four very fast eigenvalues (see last section), which are reduced using a diagonal realization. One can verify flexible mode stability on the root locus obtained with the full-order model (Fig. 3). This property is robust to the various loading cases because the synthesis model does not take into account these flexible modes. The compensator poles, located by grey × symbol, are close to the rigid plant poles. This indicates that the rolloff is in the low-frequency range; therefore, compensator and rigid plant dynamics are coupled. As a consequence, simulation results (not presented here) reveal a slight deterioration of time-domain performances in comparison to Fig. 1.

Active Synthesis

The precedings synthesis does not influence the flexible modes. This can be interpreted on the root locus by the absence of trajectories starting from the flexible modes. They are in the same location in open loop and in closed loop (Fig. 3). Thus, such a compensator cannot improve comfort during turbulence. In this section, we will seek to act on the flexible modes or more exactly to damp these modes in closed loop. To do so, we will relax the rolloff specification to increase control law bandwidth up to 3 Hz, that is,

$$r = 2, \qquad \omega = 6\pi \text{ rad/s} \tag{19}$$

The flexible modes that are sensitive in this frequency range will also be taken into account in the synthesis model. The synthesis model now corresponds to the 30th-order reduced model $G(s)$ in which 12 flexible modes are retained [see Eq. (6)]. The direct application of the earlier synthesis setup (Fig. 6) does not allow the flexible modes to be damped. The flexible states (q_j and $\dot{q}_j$, $j = 1, 3, 4, \ldots, 13$) are not weighted at the controlled outputs z_1 and z_2 due to the structure of gain K [Eq. (16)]. Therefore, it is necessary to complete the synthesis setup according to Fig. 7. The vector output z_3 directly weighs the derived states $\dot{q}_j$ of the 12 flexible modes through the static matrix N. In this manner, one can directly modify the flexible mode damping ratios by means of a static weighting ρ_s. The nominal tuning is quite simple and identically weights the flexible modes below the rolloff pulsation ω, whereas the modes just beyond this pulsation are not weighted:

$$\rho_s = \text{diag}(5, 5, 5, 5, 5, 5, 5, 5, 1, 0, 0, 0) \tag{20}$$

However, this solution is not robust with respect to the various loading cases and is sensitive to the variations in the characteristics of the flexible modes (frequencies, damping ratios); in fact, the compensator reveals some zeros on the plant flexible poles. These cancellations express the tendency of optimal synthesis techniques to inverse the plant locally. To prevent this behavior, model uncertainties should be specified in the standard problem. In this way, we chose to take into account variations on flexible mode damping ratios: the 12 inputs $\boldsymbol{w}_3$ (through the matrix M) and the 12 outputs $\boldsymbol{z}_3$ (through the matrix N) are given by the linear fractional transformation (LFT) modeling of these parametric variations, completed by static weightings ρ_e (identical on all of the modes) and ρ_s, respectively,

$$\rho_e = 0.2\, I_{12\times 12} \tag{21}$$

The LFT representation of additive variations δ_{ξ_j} on flexible mode damping ratios ξ_j can be performed in the following way.

Let A_j, B_j, and C_j be the elementary blocks associated with the flexible mode number j in the real normalized block-diagonal realization of the model:

$$A_j = \begin{bmatrix} 0 & 1 \\ -\omega_j^2 & -2\xi_j\omega_j \end{bmatrix}, \qquad B_j = \begin{bmatrix} B_j^1 \\ B_j^2 \end{bmatrix}$$

$$C_j = \begin{bmatrix} C_j^1 & C_j^2 \end{bmatrix} \tag{22}$$

then the LFT form reads:

$$\begin{bmatrix} \vdots \\ \dot{x}_j^1 \\ \dot{x}_j^2 \\ \vdots \\ \hline z_j \\ \hline \boldsymbol{y} \end{bmatrix} = \left[\begin{array}{ccccc|c|c} \ddots & & & & & \vdots & \vdots \\ & 0 & 1 & & & 0 & B_j^1 \\ & -\omega_j^2 & -2\xi_j\omega_j & & & 1 & B_j^2 \\ & & & & \ddots & \vdots & \vdots \\ \hline \cdots & 0 & 2\omega_j & \cdots & & 0 & 0 \\ \hline \cdots & C_j^1 & C_j^2 & \cdots & & 0 & 0 \end{array}\right] \begin{bmatrix} \vdots \\ x_j^1 \\ x_j^2 \\ \vdots \\ \hline w_j \\ \hline \boldsymbol{u} \end{bmatrix} \tag{23}$$

$$w_j = \delta_{\xi_j} z_j \tag{24}$$

Normalized here means that, among all of the real block-diagonal realizations, we chose the one which normalizes the input matrix B_j to

$$\begin{bmatrix} 0 \\ 1 \end{bmatrix}$$

in the single-input case. In the multi-input case, we chose

$$B_{jk} = \begin{bmatrix} 0 \\ 1 \end{bmatrix}$$

where B_{jk} is the column of matrix B_j associated with the input k that dominates the jth mode controllability.

We recognize here the PRLQG procedure,[16,17] set up into the general H_2 synthesis framework, which consists of desensitizing the synthesis by increasing ρ_e as long as the performance is not too significantly degraded. Root loci shown in Fig. 4 (light case) and 8 (heavy case) correspond to the nominal tuning, designated $K_1(s)$. We can see that flexible mode damping ratios are increased in closed loop and that this property is robust to the loading configuration.

Finally, note that the tuning of the standard problem (Fig. 7) is independent of the measurements used. This property is particularly attractive in this problem where the set of measurements can be modified. The results presented here (Figs. 4 and 8–12) were obtained with a set of six measurements (n_{y7}, n_{y9}, p_6, r_1, r_{11}, ϕ_6) selected by an analysis of modal participation factors on the measurements and their sensitivity to loading.[18]

Two-Degree-of-Freedom Compensator Synthesis by Equivalent LQG Structure

The preceding solution is interesting for its robust performance properties, particularly the robustness of the damping introduced on the flexible modes. On the other hand, the time responses presented in Fig. 9 are not satisfactory due to the overshoot of β, a non-minimum phase response on ϕ for a step in β_{ref} and a too slow a rise time for p. Thus, it is necessary to synthesize a dynamic feedforward to overcome these defects. This point is a very significant aspect in flight control design.

The approach we propose here consists of redefining the earlier output feedback as an LQG compensator.[12] This LQG compensator will involve an onboard model, which will be integrated online according to the structure shown in Fig. 10. We chose to use the rigid model here as the onboard model. The uncontrollability from $\boldsymbol{e}$ of the rigid states estimation modes leads to a dynamic feedforward effect.[19] Thus, we need not introduce additional dynamics such as with classical structures, where the feedforward path and the feedback path are uncoupled. The structure we obtain is said to be a two-degree-of-freedom compensator.

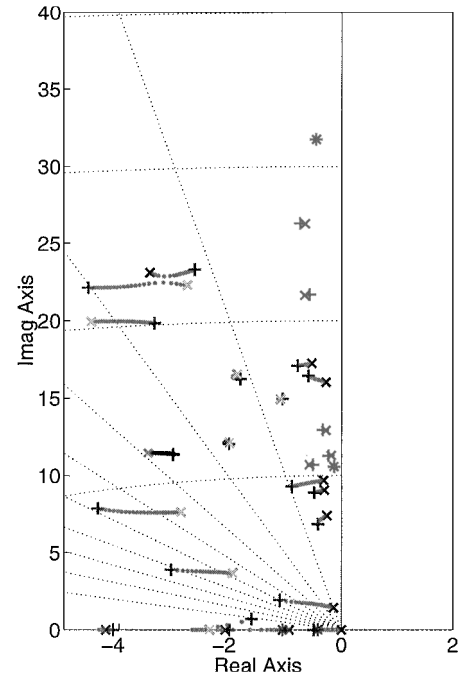

Fig. 8 $-K_1(s)G_2(s)$: root locus.

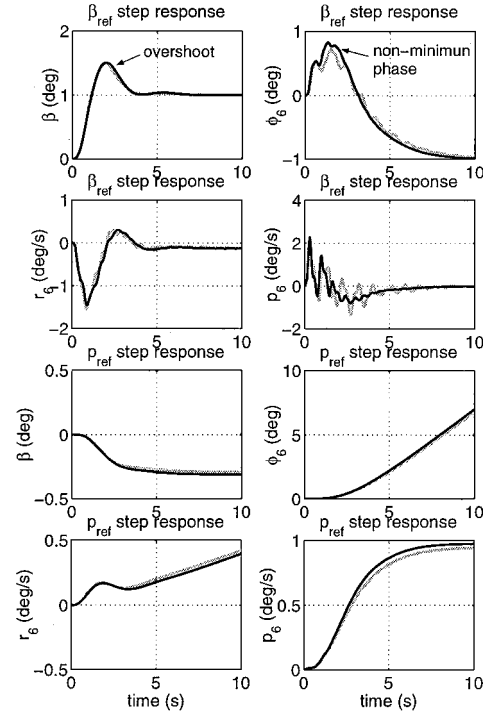

Fig. 9 Simulations: $K_1(s)$ with G_1 (black) and G_2 (gray).

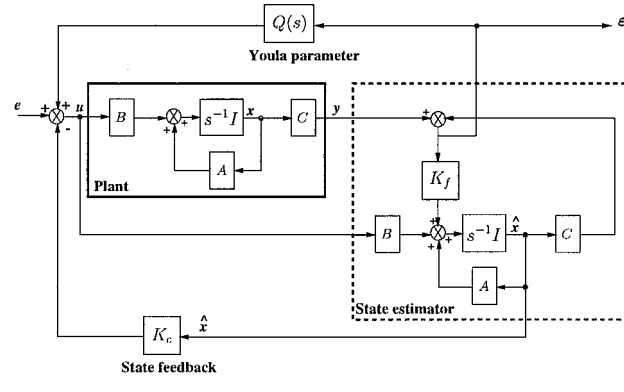

Fig. 10 YOULA parameterization with LQG structure.

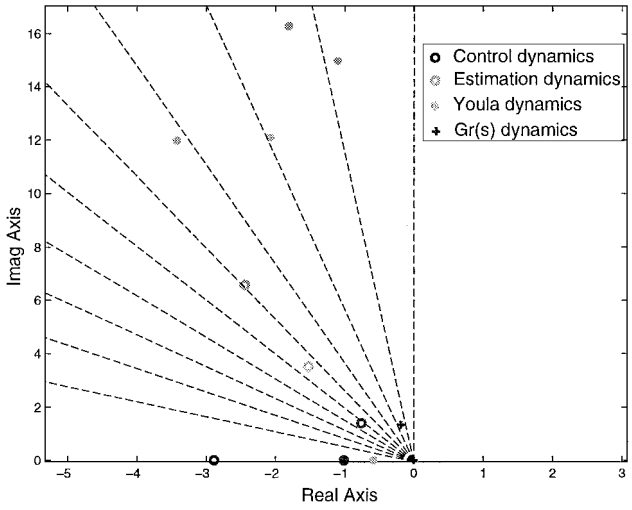

Fig. 11 Eigenvalue distribution (around rigid modes).

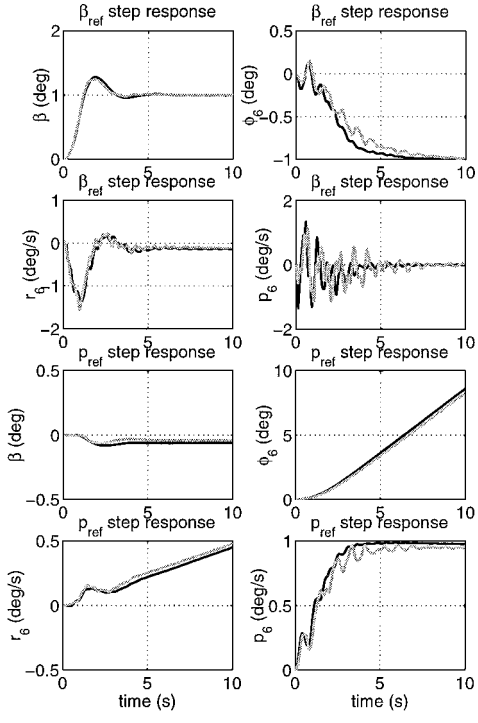

Fig. 12 Simulations with the two-degree-of-freedom equivalent LQG compensator.

An algorithm has recently been proposed[12] for the calculation of the parameters K_c, K_f, and $Q(s)$, which entirely define the compensator. Note that there are several solutions, depending on the choice of the distribution of the closed-loop eigenvalues between the state-feedback dynamics [spec$(A - BK_c)$], the state-estimation dynamics [spec$(A - K_f C)$], and the Youla parameter dynamics [[spec(A_Q)], where spec$(\cdot)$ is the set of eigenvalues. The transfer between $\boldsymbol{e}$ and $\boldsymbol{u}$, that is, the feedforward path, depends directly on this choice. The range of solutions can be reduced according to the following considerations.

1) A set of self-conjugated eigenvalues must be chosen to find a real parameterization.

2) An uncontrollable (respectively, unobservable) eigenvalue in the system must be selected in the state-feedback dynamics (respectively, state-estimation dynamics).

3) The state-estimation dynamics [spec$(A - K_f C)$] are usually chosen faster than the state-feedback dynamics [spec$(A - BK_c)$].

The nominal compensator $K_1(s)$ was first reduced to 20th order (truncation in the balanced realization) and then transformed into LQG form on the 4th-order rigid model (then, we obtain a 16th-order Youla parameter). The closed-loop eigenvalue distribution (in the vicinity of the rigid dynamics) we have chosen is shown in Fig. 11. The reference signal $\boldsymbol{e}$ really applied is

$$\boldsymbol{e} = H \begin{bmatrix} \beta_{\text{ref}} \\ \dfrac{1}{s} p_{\text{ref}} \end{bmatrix} \tag{25}$$

where H is a static feedforward matrix computed to ensure the prescribed steady state [Eq. (3)]. The simulation thus obtained is presented in Fig. 12. We can see that the overshoot on β is reduced, the nonminimum phase response on ϕ has disappeared, the roll/yaw decoupling is restored, and the settling time on p is halved. However, this improvement in response has the undesirable effect of exciting the flexible modes. Nevertheless, the transient responses now satisfy the flying quality requirements.

Conclusions

We presented a robust H_2 design and its application to the lateral flight control laws of a highly flexible aircraft. The concept of cross standard form allows roll/yaw channel decoupling to be taken into account in this frequency-domain approach, without increasing the order of the augmented plant. This design allows the parametric robustness specifications to be taken into account implicitly, but successfully. Although this design requires several steps, the tuning of each step is simple and independent of the next step in such a way that the tuning procedure is sequential. The number of tuning parameters is not too high [K_{xr} (2×4), r, ω, ρ_s, ρ_e]. Finally, the synthesis setup we proposed enables sensor location and selection to be studied from the closed-loop robustness point of view, without repeating the whole tuning process. This is certainly the most interesting property of this approach, although this property has not been fully exploited in the scope of this paper.

The equivalent LQG form technique has been used to express the compensator as a two-degree-of-freedom LQG compensator involving the rigid onboard model. The dynamic feedforward effect associated with this structure allows rigid mode transient responses to the pilot's commands to be mastered. Although the active damping produced by the control law is quite satisfactory, the flexible mode contribution to these responses is still too significant. Nevertheless, these encouraging results suggest that this technique could be applied to onboard models more realistic than the rigid model.

Acknowledgments

This work was carried out in collaboration with European Aeronautic Defense and Space Company/Airbus and with the support of Service Programme Aéronautique, Direction Générale de l'Armement.

References

[1] Balas, G., and Doyle, J., "Control of Lightly Damped, Flexible Modes in the Controller Crossover Region," *Journal of Guidance, Control, and Dynamics*, Vol. 17, No. 2, 1994, pp. 370–377.

[2] Alazard, M., Chrétien, J., and Du, M. L., "Attitude Control of a Telescope with Flexible Modes," *Dynamic and Control of Structures in Space III*, Computational Mechanics, London, 1996, pp. 167–184.

[3] Tahk, M., and Speyer, J., "Parameter Robust Linear Quadratic Gaussian Design Synthesis with Flexible Structure Control Applications," *Journal of Guidance, Control, and Dynamics*, Vol. 12, No. 3, 1989, pp. 460–468.

[4] Tischler, M. B., *Advances in Aircraft Flight Control*, Taylor and Francis, Washington, DC, 1996, pp. 211–229.

[5] Stevens, B. L., and Lewis, F. L., *Aircraft Control and Simulation*, Wiley, New York, 1992, pp. 421–437.

[6] Sato, M., and Suzuki, M., "Vibration Control of Flexible Structures Using a Combined $\mathcal{H}_\infty$ Filter Approach," *Journal of Guidance, Control, and Dynamics*, Vol. 19, No. 5, 1996, pp. 1000–1006.

[7] Joshi, S., and Kelkar, A. G., "Inner Loop Control of Supersonic Aircraft in the Presence of Aeroelastic Modes," *IEEE Transactions on Control Systems Technology*, Vol. 6, No. 6, 1998, pp. 730–739.

[8] Kubica, F., Livet, T., Le Tron, X., and Bucharles, A., "Parameter—Robust Flight Control System for a Flexible Aircraft," *Control Engineering Practice*, Vol. 3, No. 9, 1995, pp. 1209–1215.

[9] Livet, T., Fath, D., and Kubica, F., "Robust Autopilot Design for a Highly Flexible Aircraft," *13th IFAC World Congress*, Vol. P, International Federation of Automatic Control, 1996, pp. 279–284.

[10] Hicks, K. L., and Rodriguez, A. A., "Decoupling Compensation for the Apache Helicopter," *Conference on Decision and Control*, Vol. 2, Inst. of Electrical and Electronics Engineers, New York, 1996, pp. 1551–1556.

[11]Ferreres, G., and Dardenne, I., "LP Synthesis of a Lateral Flight Control System for a Transport Aircraft," *Guidance, Navigation, and Control Conference*, Vol. 1, AIAA, Reston, VA, 1997, pp. 155–164.

[12]Alazard, D., and Apkarian, P., "Exact Observer-Based Structures for Arbitrary Compensators," *International Journal of Robust and Non-Linear Control*, Vol. 9, No. 2, 1999, pp. 101–118.

[13]Madelaine, B., and Alazard, D., "Flexible Structure Model Contruction for Control System Design," *Guidance, Navigation, and Control Conference*, Vol. 2, AIAA, Reston, VA, 1998, pp. 1165–1174.

[14]Champetier, C., and Magni, J., "Analysis and Synthesis of Modal Control Laws," *Recherche Aérospatiale*, Vol. 6, 1989, pp. 17–35.

[15]Zhou, K., Doyle, J. C., and Glover, K., *Robust and Optimal Control*, Prentice–Hall, Upper Saddle River, NJ, 1996, pp. 413–439.

[16]Tahk, M., and Speyer, J., "Modeling of Parameter Variations and Asymptotic LQC Synthesis," *IEEE Transactions on Automatic Control*, Vol. AC-32, No. 9, 1987, pp. 793–801.

[17]Alazard, D., Cumer, C., Apkarian, P., Gauvrit, M., and Ferreres, G., *Robustesse et Commande Optimale*, CEPADUES Édition, Toulouse, France, 1999, pp. 189–196.

[18]Alazard, M., Bucharles, A., Ferreres, G., Magni, J. F., and Prudhomme, S., "Towards a Global Methodology for Flexible Aircraft Control," *Structural Aspect of Flexible Aircraft Control*, Research and Technology Organization, Ottawa, 1999, pp. 25.1–25.10.

[19]Franklin, G. F., and Johnson, C. R., Jr., "A Condition for Full Zero Assignment in Linear Control Systems," *IEEE Transactions on Automatic Control*, Vol. AC-26, No. 2, 1981, pp. 519–521.